Efficiency Drop in Green InGaN/GaN Light Emitting Diodes: The Role of Random Alloy Fluctuations

Matthias Auf der Maur,[1,*] Alessandro Pecchia,[2] Gabriele Penazzi,[3] Walter Rodrigues,[1] and Aldo Di Carlo[1]
[1]*Department of Electronic Engineering, University of Rome Tor Vergata, Via del Politecnico 1, 00133 Rome, Italy*
[2]*CNR-ISMN, via Salaria Km 29.300, 00017 Monterotondo, Rome, Italy*
[3]*Bremen Center for Computational Materials Science, University of Bremen, 28359 Bremen, Germany*
(Received 12 May 2014; revised manuscript received 27 October 2015; published 15 January 2016)

White light emitting diodes (LEDs) based on III-nitride InGaN/GaN quantum wells currently offer the highest overall efficiency for solid state lighting applications. Although current phosphor-converted white LEDs have high electricity-to-light conversion efficiencies, it has been recently pointed out that the full potential of solid state lighting could be exploited only by color mixing approaches without employing phosphor-based wavelength conversion. Such an approach requires direct emitting LEDs of different colors, including, in particular, the green-yellow range of the visible spectrum. This range, however, suffers from a systematic drop in efficiency, known as the "green gap," whose physical origin has not been understood completely so far. In this work, we show by atomistic simulations that a consistent part of the green gap in *c*-plane InGaN/GaN-based light emitting diodes may be attributed to a decrease in the radiative recombination coefficient with increasing indium content due to random fluctuations of the indium concentration naturally present in any InGaN alloy.

DOI: 10.1103/PhysRevLett.116.027401

III-nitride-based light emitting diodes (LEDs) have become since their breakthrough in 1993 [1] the most promising candidates for ultrahigh efficiency solid state lighting (SSL), earning Nakamura, Amano, and Akasaki last year's Noble Prize in Physics. Currently, the power conversion efficiency of blue InGaN/GaN LEDs is exceeding 80% [2], and wide adoption of ultraefficient SSL solutions would allow for substantial increase in energetic efficiency of generic lighting and to potential energy saving [3]. Usually, white light emission is obtained by partially converting the emission of a blue LED to the yellow-green spectral range by means of a phosphor. This conversion is associated with an energy loss known as Stokes' loss, which is in the order of 25% and therefore limits the highest attainable white phosphor-converted LED efficiency to well below 100% [3]. This loss mechanism can be eluded by eliminating the phosphor-based down-conversion and using direct color mixing instead, combining the light of several LEDs emitting at different wavelengths, usually blue, green, red, and possibly yellow. In fact, it has been pointed out recently that in order to exploit the full potential of SSL, it will be necessary to eventually eliminate the phosphor-based down-conversion by moving to color mixing approaches based on semiconductor-only multicolor electroluminescence [3–5]. This will allow for the highest possible efficiency in light generation, described by the internal quantum efficiency (IQE), and for smart-lighting applications requiring particular emission spectra or detailed control on color mixing [3] and for increased lifetime.

The most important issue hampering the transition to phosphor-free solutions is the "green gap." The green gap indicates a severe drop in efficiency of green-yellow emitters compared to blue and red ones [6], for III-nitride and III-phosphide technology, respectively, as shown in Fig. 1. The low efficiency of green LEDs is particularly critical, since phosphor-free white LEDs based on color mixing require at least a green emitter with wavelength around 530 nm [7], lying nearly at the center of the green gap. Therefore, the efficiency of an all-semiconductor white light source is limited by the efficiency of the green emitter, and in fact today's white phosphor-converted

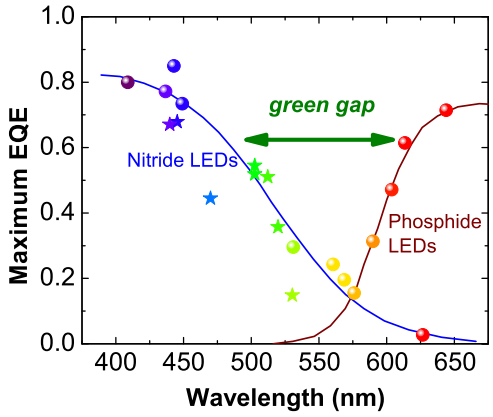

FIG. 1. The green gap. Maximum external quantum efficiency (EQE) of different commercial nitride and phosphide LEDs (spheres), illustrating the green gap problem. Data points have been taken from Ref. [7]. The lines are guides to the eye. The stars give the EQE of the nitride single-quantum-well LEDs from Ref. [8] which we have used for comparison with simulations.

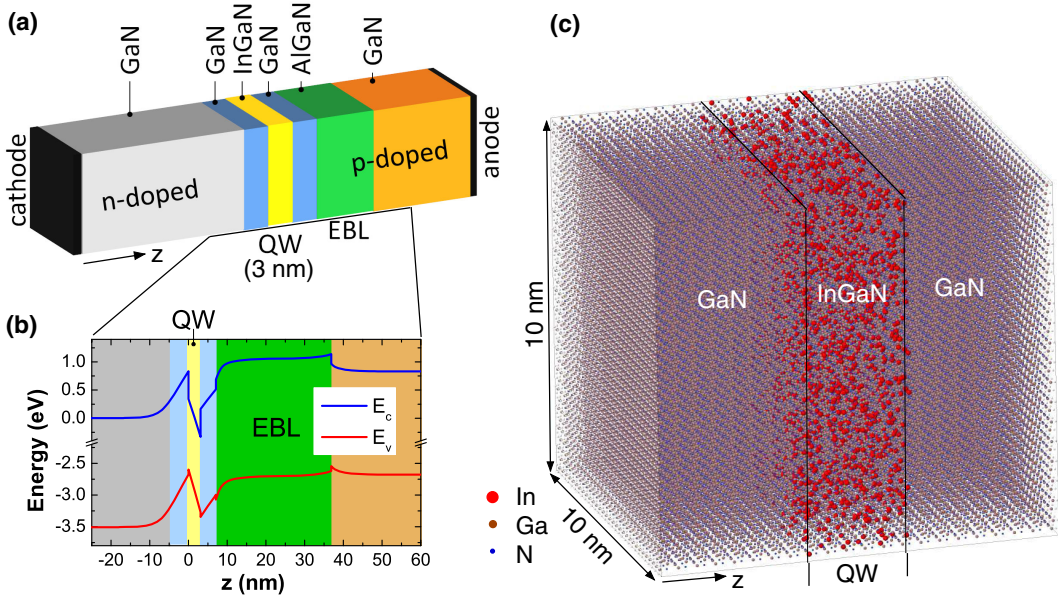

FIG. 2. Schematic structure of the simulated devices. (a) Schematic structure of the SQW LEDs used in the simulations. (b) Typical conduction and valence band edge profile near the predicted maximum IQE point (for 20% indium). (c) Atomistic structure of one random alloy sample. The red dots are the indium atoms.

LEDs have higher efficiency than green LEDs [3]. As a consequence, to reach ultraefficient white LEDs, it is of paramount importance to understand the origins of the green gap.

The most advanced technology for green LEDs is based on c-plane InGaN/GaN multi-quantum-well LEDs, as used for blue LEDs but with higher indium content in the InGaN quantum wells (QWs). To understand the green gap, it is therefore necessary to study the changes in device performance with increasing indium content.

It is known that both decreasing material quality and increasing quantum confined Stark effect (QCSE) due to the high polarization fields in c-plane InGaN/GaN QWs reduce LED efficiency at increasing indium content [8,9]. The former leads to increased nonradiative recombination, whereas the latter reduces the overlap between electron and hole wave functions and thus the associated momentum matrix elements. Recent experimental results suggest, however, that the decrease of the radiative recombination coefficient with increasing indium content is stronger than expected from QCSE alone [8]. A possible explanation for the additional decrease in radiative recombination rate could be localization of electrons and holes in the QW plane due to statistical fluctuations in the InGaN alloy [10,11]. In fact, it is known that even in a uniform alloy, random fluctuations of the local indium concentration lead to statistical spread of the electronic states's energies and partial localization of the wave functions, when calculated with atomistic models like tight binding [11–13].

To quantitatively assess the effect of alloy fluctuations on the maximum LED efficiency, we calculated the spontaneous emission properties of c-plane InGaN/GaN single-quantum-well (SQW) LEDs including an AlGaN electron blocking layer (EBL) and with indium contents between 15% and 35% and extracted the radiative recombination parameter B. This number has then been compared with experimentally determined values based on the ABC model [8,14], which describes the total recombination rate as $R = An + Bn^2 + Cn^3$, where A is the defect related Shockley-Read-Hall (SRH) recombination parameter, n is the carrier density, and the parameter C is usually interpreted as the Auger recombination coefficient. In this model, the internal quantum efficiency (IQE) is given by the ratio of radiative to total recombination, i.e., $\mathrm{IQE} = Bn^2/(An + Bn^2 + Cn^3)$. To obtain B, we calculated the confined electron and hole states and the corresponding optical transitions' momentum matrix elements (MME), using an atomistic empirical tight-binding approach [15,16] and assuming an operating point of the LED near the maximum IQE. We performed the empirical tight-binding calculations using both a homogeneous effective medium approximation (virtual crystal approximation) and a random alloy approach in order to quantify the effect of alloy fluctuations in the InGaN. For the construction of the atomic structure, we assumed a uniform random alloy, since recent experimental evidence suggests that InGaN layers of good quality should not deviate much from the ideal uniform case [17–19]. The random alloy calculations have been performed on 30 random structures for each indium content. The schematic device structure used for the simulations, a typical band diagram and a random atomistic structure, are shown in Fig. 2 for the case of 20% indium.

Figure 3(a) shows a scatter plot of the ground state MME for zero transverse momentum (i.e., at the Γ point) for the different random samples in comparison with the values obtained in effective medium approximation. We observe a linear correlation between ground state transition energy and MME, and an increasing spectral spread, confirming earlier results [10–13]. The MMEs obtained assuming an effective medium are strictly higher than the random alloy values,

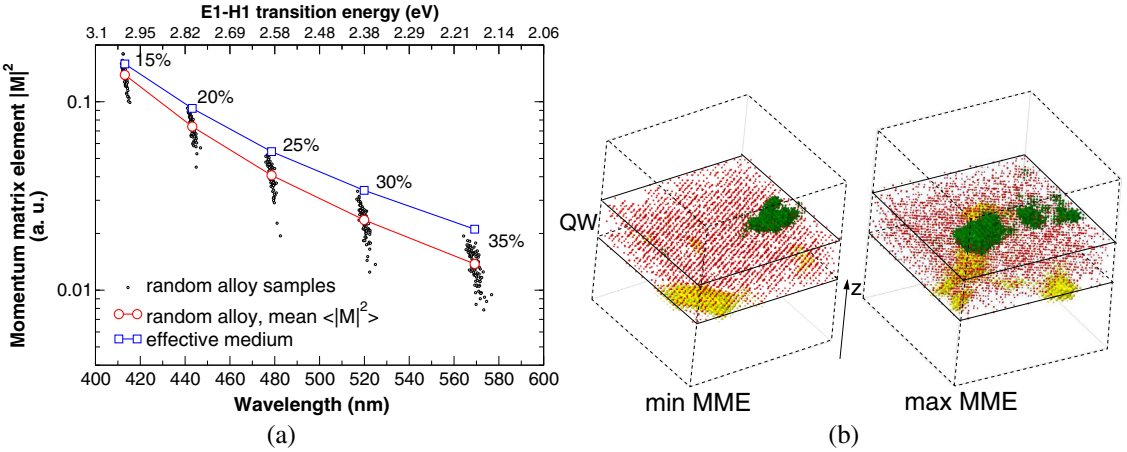

FIG. 3. Ground state momentum matrix elements and wave functions. (a) Ground state transition matrix elements in atomic units calculated at zero in-plane momentum (Γ point) using random alloy and effective medium approach, respectively. (b) Ground state electron (green) and hole (yellow) wave functions for the 30% In QW with the smallest and largest momentum matrix elements. The isosurfaces containing 10% of the total ground state density are shown. The red dots are the indium atoms.

indicating that simulations based on this assumption tend to overestimate spontaneous emission strength. The scattering of the MME can be attributed to variations in wave function overlap in the quantum well plane due to indium fluctuations [10], as shown in Fig. 3(b), where the ground state electron and hole wave functions are shown for the 30% indium QW having the smallest and largest MMEs, respectively. The strong spread in the values of the MME is due to the fact that the lateral fluctuations of the electron and hole wave functions are largely independent, since they are subject to alloy fluctuations on distant atomic planes due to spatial separation along the crystal's c axis.

For a direct comparison with experimental data, we estimated the radiative recombination coefficient B from the simulation results. For this, we calculated eight electron and eight hole states in four points of the reduced Brillouin zone and extracted the radiative recombination rates and carrier densities. From the statistical ensembles for each indium content, we calculated the mean spontaneous recombination rate $\bar{R}_{\mathrm{sp}} = 1/N \sum_i R_{\mathrm{sp},i}$ and similarly the mean electron and hole densities $\bar{n}$ and $\bar{p}$, where $R_{\mathrm{sp},i}$ are the spontaneous recombination rates for each random sample calculated by Fermi's golden rule [20] and N is the ensemble size. Then, we extracted an effective radiative recombination parameter B_{eff} defined such that $\bar{R}_{\mathrm{sp}} = B_{\mathrm{eff}} \bar{n}\, \bar{p}$. This is based on the assumption that the macroscopically observed recombination rates and carrier densities are the spatial mean values.

Based on the ABC model and using the experimentally extracted recombination coefficients, we can estimate the effect of random alloy fluctuations on the maximum IQE that can be expected from a c-plane InGaN/GaN SQW LED and, in particular, its wavelength dependence. In the ABC model, the maximum IQE is given by

$$\mathrm{IQE}_{\mathrm{max}} = B/(B + 2\sqrt{AC}). \quad (1)$$

Since in this work we are mainly interested in the effect of the wavelength dependence of B, we assumed wavelength independent A and C parameters, taking a SRH recombination coefficient $A = 7 \times 10^5\ \mathrm{s}^{-1}$ and the approximately constant Auger coefficient $C = 10^{-31}\ \mathrm{cm}^6\ \mathrm{s}^{-1}$ from Ref. [8], and calculated $\mathrm{IQE}_{\mathrm{max}}$ based on (1) at different wavelengths using both the theoretical and the experimental B parameters. This allows us to compare the theoretical and measured wavelength dependence of the maximum IQE under the best-case assumption of constant nonradiative recombination. For a quantitative comparison, we scale the simulated radiative recombination parameters by a wavelength independent constant such that at low wavelengths the predicted IQE corresponds to the measured one (see the Supplemental Material Ref. [21] for a discussion of the absolute values of B). Figure 4(a) shows the calculated IQE as a function of current density. It can be seen that uniform random alloy fluctuations lead to an additional progressive reduction of the IQE of up to roughly 0.1 with respect to the prediction based on an effective medium approximation. The trend with wavelength of the peak IQE predicted by the random alloy calculation is in good agreement with the experimental data, as shown in Fig. 4(b). We note that assuming some nonuniformity in the indium distribution does not significantly change the calculated B, whereas it substantially broadens the predicted emission spectra (see the Supplemental Material). Therefore, uniform random alloy fluctuations can be identified to give an important contribution to the green gap, and our results allow us to quantify this contribution to account for up to 30% in the green spectral region. Figure 4 also shows that the combination of nonradiative recombination, dependency of optical strength on emission energy, QCSE due to the internal field, and finally alloy fluctuations may comprehensively explain the origins of the green gap in nitride LEDs.

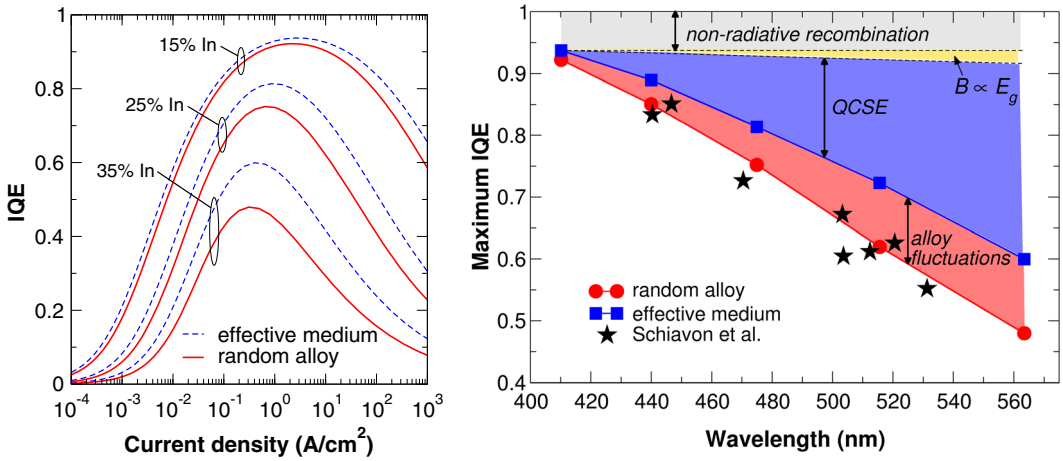

FIG. 4. Comparison of IQE between simulation and measurement. (a) Simulated IQE versus current density curves, showing the effect of random alloy fluctuations with respect to the effective medium approximation. (b) Wavelength dependency of the peak IQE as expected from simulations compared with the value obtained using the measured B. For the SRH and Auger rate coefficients, we have assumed constant values of $A = 7 \times 10^5$ s^{-1} and $C = 10^{-31}$ cm^6 s^{-1}, respectively [8]. Random alloy fluctuations induce an additional drop in IQE of up to 0.1.

In summary, based on atomistic simulations of c-plane InGaN/GaN SQW LEDs including uniform random alloy fluctuations, we predicted the radiative recombination parameter B for different mean indium contents. We have shown that the wavelength dependence of B is compatible with experimental findings and that simulation approaches based on homogeneous effective media approximations, typically used for device simulations, overestimate B by an amount proportional to the mean indium content in the QW. Comparing the predicted maximum IQE with the one obtained using measured values of B, assuming for the nonradiative recombination parameters wavelength independent values, leads to the conclusion that alloy fluctuations give rise to an important material intrinsic contribution to the green gap, which in the studied structures can be as big as 30% of the total IQE drop at green wavelengths. Since the strong scattering of the momentum matrix elements is due to the internal field induced uncorrelated lateral fluctuations of electron and hole wave functions, it can be expected that in nonpolar QWs, the effect of the random alloy fluctuations would be considerably reduced due to the absence of QCSE.

M. A. d. M., A. P., and A. D. C. conceived the study. M. A. d. M. set up and performed the simulations, analyzed the data, and wrote the manuscript. M. A. d. M., A. P., and G. P. contributed to the software implementation of the models, and W. R. parallelized the tight-binding code. All authors discussed the results and edited the manuscript. The research leading to these results has received funding from the European FP7 Project NEWLED under Grant No. 318388.

*auf.der.maur@ing.uniroma2.it

[1] Shuji Nakamura, Masayuki Senoh, and Takashi Mukai, P-GaN/N-InGaN/N-GaN double-heterostructure blue-light-emitting diodes, Jpn. J. Appl. Phys. **32**, L8 (1993).
[2] Yukio Narukawa, Masatsugu Ichikawa, Daisuke Sanga, Masahiko Sano, and Takashi Mukai, White light emitting diodes with super-high luminous efficacy, J. Phys. D **43**, 354002 (2010).
[3] Jeffrey Y. Tsao, Mary H. Crawford, Michael E. Coltrin, Arthur J. Fischer, Daniel D. Koleske, Ganapathi S. Subramania, G. T. Wang, Jonathan J. Wierer, and Robert F. Karlicek, Toward smart and ultra-efficient solid-state lighting, Adv. Opt. Mater. **2**, 809 (2014).
[4] H. Jeong, H. J. Jeong, H. M. Oh, C.-H. Hong, E.-K. Suh, G. Lerondel, and M. S. Jeong, Carrier localization in In-rich InGaN/GaN multiple quantum wells for green light-emitting diodes, Sci. Rep. **5**, 9373 (2015).
[5] K. P. O'Donnell, M. Auf der Maur, A. Di Carlo, K. Lorenz, and the SORBET Consortium, It's not easy being green: Strategies for all-nitrides, all-colour solid state lighting, Phys. Status Solidi RRL **6**, 49 (2012).
[6] Elaine Taylor, Paul R. Edwards, and Robert W. Martin, Colorimetry and efficiency of white LEDs: Spectral width dependence, Phys. Status Solidi (a) **209**, 461 (2012).
[7] K. A. Bulashevich, A. V. Kulik, and S. Y. Karpov, Optimal ways of colour mixing for high-quality white-light LED sources, Phys. Status Solidi (a) **212**, 914 (2015).
[8] D. Schiavon, M. Binder, M. Peter, B. Galler, P. Drechsel, and F. Scholz, Wavelength-dependent determination of the recombination rate coefficients in single-quantum-well GaInN/GaN light emitting diodes, Phys. Status Solidi (b) **250**, 283 (2013).
[9] Y. Zhao, S. H. Oh, F. Wu, Y. Kawaguchi, S. Tanaka, K. Fujito, J. S. Speck, S. P. DenBaars, and Shuji Nakamura, Green semipolar (20$\bar{2}$ $\bar{1}$) InGaN light-emitting diodes with

small wavelength shift and narrow spectral linewidth, Appl. Phys. Express **6**, 062102 (2013).
[10] S. Karpov, ABC-model for interpretation of internal quantum efficiency and its droop in III-nitride LEDs: a review, Opt. Quantum Electron. **47**, 1293 (2015).
[11] Stefan Schulz, Miguel A. Caro, Conor Coughlan, and Eoin P. O'Reilly, Atomistic analysis of the impact of alloy and well-width fluctuations on the electronic and optical properties of InGaN/GaN quantum wells, Phys. Rev. B **91**, 035439 (2015).
[12] M. Lopez, A. Pecchia, M. Auf der Maur, F. Sacconi, G. Penazzi, and A. Di Carlo, Atomistic simulations of InGaN/GaN random alloy quantum well LEDs, Phys. Status Solidi (c) **11**, 632 (2014).
[13] Miguel A. Caro, Stefan Schulz, and Eoin P. O'Reilly, Theory of local electric polarization and its relation to internal strain: Impact on polarization potential and electronic properties of group-III nitrides, Phys. Rev. B **88**, 214103 (2013).
[14] S. Karpov, in *Proceedings of the International Conference on Numerical Simulation of Optoelectronic Devices, NUSOD* (2014), p. 17, doi: 10.1109/NUSOD.2014.6935334.
[15] J.-M. Jancu, R. Scholz, F. Beltram, and F. Bassani, Empirical $spds^{\star}$ tight-binding calculation for cubic semiconductors: General method and material parameters, Phys. Rev. B **57**, 6493 1998.
[16] J. M. Jancu, F. Bassani, F. Della Sala, and R. Scholz, Transferable tight-binding parametrization for the group-III nitrides, Appl. Phys. Lett. **81**, 4838 (2002).
[17] S. Kret, P. Dłużewski, A. Szczepańska, M. Żak, R. Czernecki, M. Kryśko, M. Leszczyński, and G. Maciejewski, Homogenous indium distribution in InGaN/GaN laser active structure grown by LP-MOCVD on bulk GaN crystal revealed by transmission electron microscopy and x-ray diffraction, Nanotechnology **18**, 465707 (2007).
[18] M. J. Galtrey, R. A. Oliver, M. J. Kappers, C. J. Humphreys, P. H. Clifton D. Larson, D. W. Saxey, and A. Cerezo, Three-dimensional atom probe analysis of green- and blue-emitting InGaN/GaN multiple quantum well structures, J. Appl. Phys. **104**, 013524 (2008).
[19] K. H. Baloch, A. C. Johnston-Peck, K. Kisslinger, E. A. Stach, and S. Gradecak, Revisiting the In-clustering question in InGaN through the use of aberration-corrected electron microscopy below the knock-on threshold, Appl. Phys. Lett. **102**, 191910 (2013).
[20] S. L. Chuang, *Physics of Optoelectronic Devices*, Wiley Series in Pure and Applied Optics, 1st ed. (Wiley, Hoboken, 1995).
[21] See Supplemental Material at http://link.aps.org/supplemental/10.1103/PhysRevLett.116.027401, which includes Refs. [22–41], for details on the simulation models, for a discussion of the choice of statistic ensemble size and number of states, and for additional results.
[22] S. L. Chuang and C. S. Chang, $\mathbf{k}\cdot\mathbf{p}$ method for strained wurtzite semiconductors, Phys. Rev. B **54**, 2491 (1996).
[23] D. Camacho and Y. M. Niquet, Application of Keating's valence force field model to non-ideal wurtzite materials, Physica B (Amsterdam) **42E**, 1361 (2010).
[24] W. Rodrigues, A. Pecchia, M. Auf der Maur, and A. Di Carlo, A comprehensive study of popular eigenvalue methods employed for quantum calculation of energy eigenstates in nanostructures using GPUs, Journal of Computational Electronics **14**, 593 (2015).
[25] M. Auf der Maur, G. Penazzi, G. Romano, F. Sacconi, A. Pecchia, and A. Di Carlo, The multiscale paradigm in electronic device simulation, IEEE Trans. Electron Devices **58**, 1425 (2011).
[26] M. Povolotskyi and A. Di Carlo, Elasticity theory of pseudomorphic heterostructures grown on substrates of arbitrary thickness, J. Appl. Phys. **100**, 063514 (2006).
[27] Siegfried Selberherr, *Analysis and Simulation of Semiconductor Devices*, 1st ed. (Springer-Verlag, Wien, 1984).
[28] Carlo de Falco, Emilio Gatti, Andrea L. Lacaita, and Riccardo Sacco, Quantum-corrected drift-diffusion models for transport in semiconductor devices, J. Comput. Phys. **204**, 533 (2005).
[29] Matthias Auf der Maur, Alessandro Pecchia, Gabriele Penazzi, Fabio Sacconi, and Aldo Di Carlo, Coupling atomistic and continuous media models for electronic device simulation, Journal of Computational Electronics **12**, 553 (2013).
[30] I. Vurgaftman and J. R. Meyer, Band parameters for nitrogen-containing semiconductors, J. Appl. Phys. **94**, 3675 (2003).
[31] A. Ern and J.-L. Guermond, *Theory and Practice of Finite Elements*, Springer Series in Applied Mathematical Sciences Vol. 159 (Springer, New York, 2004).
[32] L. C. Lew Yan Voon and M. Willatzen, *The k*p Method: Electronic Properties of Semiconductors* (Springer, New York, 2009).
[33] P. N. Keating, Effect of invariance requirements on the elastic strain energy of crystal with application to the diamond structure, Phys. Rev. **145**, 637 (1966).
[34] J. C. Slater and G. F. Koster, Simplified LCAO method for the periodic potential problem, Phys. Rev. **94**, 1498 (1954).
[35] P. Vogl, P. Kjalmarson, and J. D. Dow, Semi-empirical tight-binding theory of the electronic structure of semiconductors, J. Phys. Chem. Solids **44**, 365 (1983).
[36] B. A. Foreman, Consequences of local gauge symmetry in empirical tight-binding theory, Phys. Rev. B **66**, 165212 (2002).
[37] Matthias Auf der Maur, Multiscale approaches for the simulation of InGaN/GaN LEDs, Journal of Computational Electronics **14**, 398 (2015).
[38] D. M. Graham, A. Soltani-Vala, P. Dawson, M. J. Godfrey, T. M. Smeeton, J. S. Barnard, M. J. Kappers, C. J. Humphreys, and E. J. Thrush, Optical and microstructural studies of InGaN/GaN single-quantum-well structures, J. Appl. Phys. **97**, 103508 (2005).
[39] Y. Kawakami, S. Suzuki, A. Kaneta, M. Funato, A. Kikuchi, and K. Kishino, Origin of high oscillator strength in green-emitting InGaN/GaN nanocolumns, Appl. Phys. Lett. **89**, 163124 (2006).
[40] T.-J. Yang, R. Shivaraman, J. S. Speck, and Y.-R. Wu, The influence of random indium alloy fluctuations in indium gallium nitride quantum wells on the device behavior, J. Appl. Phys. **116**, 113104 (2014).
[41] Y.-M. Niquet and C. Delerue, Band offsets, wells, and barriers at nanoscale semiconductor heterojunctions, Phys. Rev. B **84**, 075478 (2011).